

## Stochastic dynamics of gravity in one dimension

Kenneth R. Yawn, Bruce N. Miller, and Willard Maier

*Department of Physics, Texas Christian University, Fort Worth, Texas 76129*

(Received 6 April 1995)

The observed relaxation time for the one-dimensional self-gravitating system (OGS) has recently been shown to be much longer than was anticipated. In this paper, a stochastic model (diffusion) of the acceleration and velocity of a labeled particle in the OGS is used to provide a method for studying the exploration of the phase space of the system by a single system member. The stochastic assumption leads to a theory of fluctuations of the discrete system away from mean field (Vlasov) dynamics. These fluctuations are studied in a series of dynamical simulations and compared to those predicted by the theory. The results compare well for system members of low energy but fail for higher energies. The magnitude of the fluctuations grows much more rapidly in the theoretical predictions than in the dynamical simulations, suggesting the existence of slow modes of relaxation.

PACS number(s): 05.40.+j, 98.10.+z

### I. INTRODUCTION

A central problem for stellar dynamics is the determination of the time scale for the relaxation of an isolated, gravitationally bound system, such as a galaxy or globular cluster. For more than two decades one-dimensional self-gravitating systems have been used as a simple model to study relaxation in gravitating systems. Computer simulations of these systems show that they tend to progress through various quasiequilibrium states as they evolve from arbitrary initial conditions. These quasiequilibrium states often last for very long times, and are approximately stationary. Recent dynamical simulations have demonstrated that the relaxation time from arbitrary initial conditions is orders of magnitude greater than anticipated by theory, and thus casts doubt on many theoretical models.

The one-dimensional self-gravitating system (OGS) has been suggested as a model for the motion of stars perpendicular to the plane of a highly flattened galaxy [1]. Others have used the system to study Lynden-Bell's theory of violent relaxation [2], the usefulness of Vlasov theory for systems with a large number of constituents [3], or to investigate ergodicity and relaxation toward equilibrium for gravitational systems [4]. The long range nature of the gravitational force complicates the study of the statistics and dynamics of gravitational systems. Each particle continuously "feels" all the other particles in the system, making gravitational systems fundamentally different than systems with short range interactions. The difficulty involved in studying large systems has generally led one to a statistical approach.

In order to learn if, how, and when the OGS evolves to equilibrium much work has been done in studying the dynamics of small to medium sized systems looking for evidence of strong ergodic behavior which would result in eventual thermal equilibrium [4,5]. The study of Lyapunov exponents and the decay of correlations in time have been used in attempts to determine when and if

thermalization occurs. A positive Lyapunov exponent would guarantee the existence of a mechanism for the OGS to come to equilibrium in a finite time starting from arbitrary initial conditions if the energy hypersurface has a single ergodic component.

Although these methods are very useful, their application to large systems is problematic. An alternative method for investigating relaxation is through the introduction of a stochastic assumption which leads to a diffusion model for the system evolution. The extent to which the stochastic model is able to accurately predict properties of the real system may provide insight into the ergodic behavior of these systems and how they may come to equilibrium. Strong ergodic properties are the *source* of stochastic phenomena. In addition, the assumption should result in the establishment of bounds for relaxation times. The ability of a diffusion model to represent the system outside of equilibrium might lend itself well to the study of the OGS moving toward equilibrium.

Brownian motion is a cornerstone of modern nonequilibrium statistical physics and is a classic example of a diffusion process. In it, a massive particle is surrounded by a fluid made up of much smaller particles (atoms). As the fluid atoms collide randomly with the heavy particle, the velocity of the heavy particle experiences discrete random jumps. Since the fluid atoms are so much lighter than the heavy particle, each macroscopic movement of the heavy particle is actually the average of many small collisions with the fluid particles. The probability of the macroscopic velocity of the heavy particle having a specific value in the next time interval will depend at most on its current velocity. With this *Markov* property, in the limit of small jumps the velocity process will become a continuous function of time and can be modeled as a diffusion whose transition probability satisfies a *Fokker-Planck* (FP) equation. The basic diffusion equation describing the Brownian process was first derived by Einstein [6]. His ideas were later generalized by Smoluchowski, Fokker, Planck, Ornstein, and others [7].

Now consider the discrete one-dimensional gravitating system made up of  $N$  sheets. The velocity of each particle is a continuous function of time. However, when two sheets cross, their accelerations experience a finite jump. In the limit that  $N \rightarrow \infty$  the size of the jumps in the acceleration vanishes as  $1/N$  and the crossing rate increases as  $N$ . Both the acceleration and velocity are needed to describe the system dynamics because the probability of two sheets crossing will also depend on the sheets' current velocity. Using this ansatz, it might be possible to model the acceleration and velocity process as a diffusion if it is also Markov. A Markov assumption should model the most rapid movement toward relaxation that the actual system could possibly realize, thereby giving a lower bound for the relaxation time, since it ignores memory effects which may constrain the evolution.

Miller [8] recently used these ideas to derive a Fokker-Planck equation that describes the drift of a particle away from ideal Vlasov behavior in equilibrium. Using the canonical ensemble, and assuming that sheet crossings occur at random times, he was able to model the evolution of the  $(a, v)$  [(acceleration, velocity)] pair as Markov. He then showed that in the Vlasov limit the  $(a, v)$  process was also Markov and that the equations of motion governing the process were deterministic. To account for the finite size and discreteness of a real system the fluctuations must be scaled up to be observable for asymptotically large  $N$ . Miller then showed that the evolution of these scaled fluctuations of the acceleration and velocity from their deterministic limits was governed by a Fokker-Planck equation with time-dependent drift and diffusion tensors [9,10]. In that initial paper the predictions of the model were not investigated.

The purpose of this paper is twofold. The first is to formulate a more general approach that will allow the study of other stationary distributions, besides equilibrium, that obey Vlasov dynamics (e.g., the waterbag distribution) where a complete canonical description, that includes interparticle correlations, is lacking. The second objective is to test the theoretical predictions of the stochastic model against the results of numerically accurate dynamical simulations. For a general stationary distribution the equivalent of a canonical ensemble for equilibrium is not available. In this paper we build the  $N$ -particle distribution function from singlet distribution functions by assuming (1) the complete phase space distribution function has no initial correlations between particles for systems of large  $N$  and (2) the particles remain statistically independent (i.e., the  $N$ -particle distribution function is completely separable) at all times. This is equivalent to beginning with the most stochastic model possible. The assumption of statistical independence (stosszahlansatz) has been proven for discrete systems in equilibrium in the limit of large  $N$  [11].

Starting with the assumption of statistical independence we obtain very general forms for the crossing rates, infinitesimal increments, and Fokker-Planck equations that govern the  $(a, v)$  process. The general FP equation for the  $(a, v)$  process has no diffusion term and therefore describes the deterministic motion of a particle in the Vlasov potential. A general FP equation with a nonzero

diffusion term is then derived for scaled up variables that describe the drift of a particle away from its Vlasov image. In principle, any stationary Vlasov distribution function can then be substituted into the general forms to give explicit equations that govern the evolution of the scaled and unscaled  $(a, v)$  processes for that system.

Next, to confirm the validity of the general equations, the equilibrium distribution function (in the Vlasov limit) is substituted into the general equations which then reduce to those obtained earlier from the canonical ensemble [8]. The resulting equations again show that the scaled fluctuations representing a particle's drift from ideal Vlasov behavior are a diffusion that obey a Fokker-Planck equation with time-dependent drift and diffusion tensors.

The theoretical predictions of the stochastic model are investigated by integrating the coupled differential equations governing the moments of the Markov state variables which are induced by the FP equation. The time-dependent behavior of the moments of the scaled process gives a theoretical prediction of the growth of the fluctuations in time. These quantities can be easily tracked throughout the course of a dynamical simulation and compared with the theory.

Finally, in order to check the validity of the theory, we describe repeated numerical simulations of a system of  $N = 1000$  particles in which the fluctuations in time of a labeled sheet are recorded and compared to that predicted by theory. The initial acceleration and velocity of the test sheet are given specific values that correspond to either a relatively high or low particle energy in the system. Comparison of the theoretical predictions with the results of the simulations shows good agreement for lower energy particles in the system. The magnitude of the theoretical fluctuations for higher energy particles appears to grow much more rapidly than for those in the simulations. This discrepancy may indicate the existence of collective modes that are not accounted for in the stochastic model.

## II. DESCRIPTION OF THE SYSTEM

The discrete one-dimensional gravitating system is a collection of  $N$  planar sheets of constant mass density  $\sigma$  infinite in, say, the  $y$  and  $z$  directions that can move along the  $x$  direction under their mutual gravitational attraction. Only gravitational forces are considered, thus the sheets do not collide but merely pass through (cross) one another. Since all sheets have the same mass density, during a crossing the sheets simply exchange accelerations and therefore experience a discrete jump, while the sheet velocities remain continuous functions of time. Between crossings the sheets simply undergo uniform acceleration produced by the inhomogeneity of the mass distribution. Because the system is isolated, momentum conservation allows us to fix the center of mass and set the total momentum to zero. The acceleration experienced by the  $j$ th sheet from the left depends only on the difference between the number of sheets (mass) to the right and the left and is given by

$$A_j = 2\pi G\sigma(N - 2j + 1), \quad (1)$$

where  $G$  is the universal gravitational constant. The energy of a system of sheets is constant and is given by

$$E = \frac{1}{2}\sigma \sum_{j=1}^N v_j^2 + 2\pi G\sigma^2 \sum_{j<i} |x_i - x_j|, \quad (2)$$

where  $v_j$  and  $x_j$  are the velocity and position of the  $j$ th sheet, respectively. If the particles are ordered and labeled consecutively from left to right (i.e.,  $x_{j+1} > x_j$ ) the energy can then be expressed as

$$E = \frac{1}{2}\sigma \sum_{j=1}^N v_j^2 + 2\pi G\sigma^2 \sum_{j=1}^{N-1} j(N-j)(x_{j+1} - x_j). \quad (3)$$

To see this, consider the work done by gravity in reducing the distance  $x_{j+1} - x_j$  to zero while keeping the distance between all other sheets constant. This work is equivalent to bringing two sheets together of mass  $j\sigma$  and  $(N-j)\sigma$  (i.e., the mass on the left and the right). Repeat this process for each pair of sheets until all the sheets are coincident. The potential energy is given by the sum of those terms, and the total energy is that shown in (3). It is customary to define the characteristic period of a sheet in the system as  $t_c = (G\rho_0/\pi)^{-1/2}$ , where  $\rho_0$  is the equilibrium mass density evaluated at the origin. This represents a typical period of oscillation of a particle in the system.

Some of the basic equilibrium properties of the one-dimensional gravitating systems were derived by Rybicki [12]. In his paper, Rybicki derives the single-particle equilibrium distribution function using both the canonical and microcanonical ensembles. Because the potential energy is a homogeneous function of the coordinates of first degree, all dependence on parameters can be removed by introducing convenient units as follows [12]:

$$L_0 = \frac{2E}{3\pi GM^2}, \quad V_0 = \left[ \frac{4E}{3M} \right]^{1/2}, \quad (4)$$

$$T_0 = \left[ \frac{1}{\pi MG} \right] \left[ \frac{E}{3M} \right]^{1/2},$$

where  $L$  is length,  $V$  is velocity,  $T$  is time,  $G$  is the universal gravitational constant, and  $E$  and  $M$  are the total system energy and mass, respectively. Dimensionless units of acceleration, velocity, position, and time are then given by

$$A \rightarrow a = \frac{A}{2\pi MG}, \quad V \rightarrow v = \frac{V}{2} \left[ \frac{3M}{E} \right]^{1/2}, \quad (5)$$

$$X \rightarrow x = \left[ \frac{3\pi GM^2}{2E} \right] X, \quad t \rightarrow \tau = \frac{t}{T_0}.$$

We will adopt these units in the remainder of the paper.

Obviously, the system can also be viewed as a collection of particles (mass points) moving in one dimension, each of mass  $m = 1/N$ , where  $m$  replaces  $\sigma$  in Eqs. (1)–(3), and we will use this language freely. In dimensionless units the acceleration of the  $j$ th particle with the ordered labeling is

$$a_j = \frac{1}{N}(N - 2j + 1). \quad (6)$$

Therefore, in specifying the particle number, we uniquely define the acceleration of that particle and vice versa. The motion of the particles is determined by both the acceleration and velocity; therefore the natural state space of the system is the  $(a, v)$  space.

In the Vlasov limit the total energy and mass of the system are held constant while the number of particles in the system is allowed to approach infinity. The probability density in  $\mu = (x, v)$  space of the resulting continuous fluid satisfies the Vlasov equation,

$$\frac{\partial f}{\partial t} = -v \frac{\partial f}{\partial x} - a \frac{\partial f}{\partial v}. \quad (7)$$

This equation is known to have an uncountably infinite number of stationary solutions [13]. In this limit, the velocity and position equilibrium distribution functions reduce to

$$\theta(v) = \pi^{-1/2} \exp(-v^2) \quad (\text{velocity}), \quad (8)$$

$$\rho(x) = \frac{1}{2} \text{sech}^2(x) \quad (\text{position}),$$

where  $x$  and  $v$  are in dimensionless units.

### III. MARKOV PROCESS

In the OGS consisting of  $N$  discrete particles, the velocity ( $v$ ) of each particle is a continuous function of time. However, when two sheets cross, their accelerations ( $a$ ) experience a finite jump. As the number of particles tends to infinity, the size of the jumps in the acceleration vanishes as  $1/N$  and the crossing rate increases as  $N$ . By assuming that the  $(a, v)$  process for a single sheet in the system is Markov in the large  $N$  limit, the jumps in the acceleration should go over to a continuous (diffusion) process. One may be tempted to model the acceleration process alone as Markov without the velocity. However, because the transition probability also depends on the velocity, this approach would not accurately model the system dynamics. The diffusion process will be completely defined by the first and second order infinitesimal increments which give the average change of a quantity in a small time interval. To calculate the increments for the  $(a, v)$  process the transition probabilities, and thus the crossing rates, are required.

#### A. Derivation of the general crossing rates

In order to calculate the infinitesimal increments of the  $(a, v)$  process, we have to first find the transition probabilities of the jump process, and these will depend on the crossing rates. In this section we will derive very simple expressions for the crossing rates that depend only on  $N$  and the singlet distribution function  $f$  in the limit of large  $N$ .

The procedure will be the following: We start with the ordered system with the condition for a crossing and average over the phase space while conditioning on the initial acceleration and velocity of the labeled particle. For the discrete system, the position of the test particle

will not be fixed by the value of the acceleration but instead will be distributed about a most probable value,  $\omega$ . The crossing rates depend on this distribution, which is sharply peaked in the limit of large  $N$ . Expanding expressions in the crossing rates and canceling terms that differ by no more than order  $(1/N)$ , we obtain expressions for the crossing rates that depend only on  $N$  and  $f$ .

The crossing rates for a labeled particle in the OGS depend on  $f$ , which depends explicitly on the acceleration (position) and velocity. No assumption about equilibrium will be made for the derivation, only the assumption of statistical independence of the particles in phase space. Monaghan and Fukita and Morita [11] have shown that this assumption is valid specifically for the equilibrium OGS in the limit of large  $N$ . Braun and Hepp [14] have shown this to be true for a wider class of systems with smooth interactions even when equilibrium is absent. With this assumption, the  $N$ -particle phase space distribution function can be expressed as

$$f^{(N)}(\mu_1, \mu_2, \dots, \mu_N) = f(\mu_1)f(\mu_2) \cdots f(\mu_N), \quad (9)$$

where  $\mu_i = (x_i, v_i)$ . For the OGS which has no "collisions," only crossings, the singlet distribution function

$f(x, v)$  will satisfy the Vlasov (or collisionless Boltzmann) equation for mass conservation (7) in the limit  $N \rightarrow \infty$ . For finite but large  $N$  the Vlasov assumption will not hold exactly, but should provide a good approximation since changes in the acceleration and velocity will be small. The requirement for a particle in the system to have a crossing with another particle from the right {left} in a small time  $\Delta t$  is

$$(v_j - v_{j+1})\Delta t > (x_{j+1} - x_j), \quad (10)$$

$$\{(v_{j-1} - v_j)\Delta t > (x_j - x_{j-1})\},$$

where the  $x_j, x_{j+1}$ , etc. refer to particle positions in the ordered system. The probability of having a crossing is found by conditioning on the initial acceleration and velocity of the test particle and averaging the requirement for a crossing over the  $2N$ -dimensional phase space. Thus the expression for the probability of a crossing from the right for the  $j$ th particle with velocity ( $v$ ) and acceleration ( $a$ ) is

$$P_r \Delta t = \langle \Theta[\Delta t(v_j - v_{j+1}) - (x_{j+1} - x_j)] | a, v \rangle. \quad (11)$$

Making use of (9) and expanding the expression we obtain

$$P_r \Delta t = \frac{\int_{-\infty}^{\infty} dx_1 \int_{-\infty}^{\infty} dv_1 \cdots \int_{-\infty}^{\infty} dx_N \int_{-\infty}^{\infty} dv_N \prod_{k=1}^{N-1} \Theta(x_{k+1} - x_k) f(\mu_k) f(\mu_N) \delta(v_j - v) \Theta[\Delta t(v_j - v_{j+1}) - (x_{j+1} - x_j)]}{\int_{-\infty}^{\infty} dx_1 \int_{-\infty}^{\infty} dv_1 \cdots \int_{-\infty}^{\infty} dx_N \int_{-\infty}^{\infty} dv_N \prod_{k=1}^{N-1} \Theta(x_{k+1} - x_k) f(\mu_k) f(\mu_N) \delta(v_j - v)}$$

$$= \frac{\int_{-\infty}^{\infty} dx_j \int_{-\infty}^{x_j} \rho(x_{j-1}) dx_{j-1} \cdots \int_{-\infty}^{x_2} \rho(x_1) dx_1 f(x_j, v) \int_{-\infty}^v f(x_j, v') (v - v') dv'}{\int_{-\infty}^{\infty} dx_j \int_{-\infty}^{x_j} \rho(x_{j-1}) dx_{j-1} \cdots \int_{-\infty}^{x_2} \rho(x_1) dx_1 f(x_j, v) \int_{x_j}^{\infty} \rho(x_{j+1}) dx_{j+1}}$$

$$\times \frac{\int_{x_j}^{\infty} \rho(x_{j+2}) dx_{j+2} \int_{x_{j+2}}^{\infty} \rho(x_{j+3}) dx_{j+3} \cdots \int_{x_{N-1}}^{\infty} \rho(x_N) dx_N}{\int_{x_{j+1}}^{\infty} \rho(x_{j+2}) dx_{j+2} \int_{x_{j+1}}^{\infty} \rho(x_{j+3}) dx_{j+3} \cdots \int_{x_{N-1}}^{\infty} \rho(x_N) dx_N}, \quad (12)$$

where the mass density

$$\rho(x_j) = \int_{-\infty}^{\infty} f(x_j, v_j) dv_j \quad (13)$$

and we have (1) introduced step functions to fix the ordering, and (2) introduced a  $\delta$  function as a condition on the velocity ( $v$ ). A similar expression holds for a crossing from the left. In (12), the step functions in  $x_k$  restrict the range of integration for the position of each particle. The symmetry of the phase space distribution under the exchange of particle coordinates admits the rearrangement of the integration order in both the numerator and denominator. This symmetry allows for the following simplification:

$$\int_x^{\infty} dx_1 \int_{x_1}^{\infty} dx_2 \cdots \int_{x_{v-1}}^{\infty} dx_v \prod_1^v \rho(x_j)$$

$$= \frac{1}{v!} \left[ \int_x^{\infty} \rho(x') dx' \right]^v = \frac{1}{v!} [M_r(x)]^v. \quad (14)$$

A similar expression holds for  $M_l(x)$ , the integrals on the left side of  $j$ .  $P_r$  then becomes

$$P_r = \frac{\int_{-\infty}^{\infty} dx f(x, v) F_{j-1, N-j-1}(x) \int_{-\infty}^v f(x, v) (v - v') dv'}{\int_{-\infty}^{\infty} dx f(x, v) F_{j-1, N-j}(x)} \quad (15)$$

where

$$F_{n,m}(x) = \frac{[M_l(x)]^n [M_r(x)]^m}{n!m!} \quad (16)$$

and we have canceled the  $\Delta t$  terms for convenience. The probability distribution in  $x$  of a particle with a given acceleration is simply  $F_{n,m}(x)$ . Thus, for finite  $N$ , the acceleration does not fix the position of the particle, and we find contributions to  $P_r$  from all  $x$ . However, taking the limit of large  $N$  with  $\alpha = j/N$  fixed ( $0 < \alpha < 1$ ) results in a sharp maximum for  $F_{n,m}$ . Let  $\omega$  and  $\omega'$  denote the values

of  $x$  which, respectively, maximize the numerator and denominator of (15). Since  $F_{n,m}(x)$  is varying rapidly near  $\omega$ , we expand  $\ln[F_{n,m}(x)]$  about its maximum and use  $M_r(x) = 1 - M_l(x)$  to give

$$\begin{aligned} M_l(\omega) &= \frac{n}{m+n} = \int_{-\infty}^{\omega} \rho(x) dx, \\ M_r(\omega) &= \frac{m}{m+n} = \int_{\omega}^{\infty} \rho(x) dx. \end{aligned} \quad (17)$$

$F_{n,m}(x)$  now becomes

$$F_{n,m}(x) \cong F_{n,m}(\omega) \exp \left[ \frac{-\frac{1}{2}(x-\omega)^2 \rho^2(\omega)(n+m)^3}{nm} \right]. \quad (18)$$

With appropriate normalization, the Gaussian approximates a  $\delta$  function in the limit of large  $N$ . Therefore

$$F_{n,m}(x) = F_{n,m}(\omega) \delta(x-\omega) \left[ \frac{2\pi nm}{\rho^2(\omega)(n+m)^3} \right]^{1/2}. \quad (19)$$

A similar expression is obtained for the denominator.

$$\begin{aligned} F_{n,m+1}(x) &= F_{n,m+1}(\omega') \delta(x-\omega') \\ &\times \left[ \frac{2\pi n(m+1)}{\rho^2(\omega')(n+m+1)^3} \right]^{1/2}. \end{aligned} \quad (20)$$

As  $N$  becomes large, the distribution about  $\omega$  becomes sharper until, in the limit,  $x$  is fixed at  $\omega$ . For finite  $N$ , however, these results will be only approximate and may cause problems for particles in the wings of the distribution where the particle density  $\rho(\omega)$  is low.

Note that in the large  $N$  limit,  $\omega \approx \omega'$ . Thus, completing the integration and canceling terms which differ by no more than order  $(1/N)$ , we finally obtain

$$\begin{aligned} P_r &= N \int_{-\infty}^v f(\omega, v')(v-v') dv', \\ P_l &= N \int_v^{\infty} f(\omega, v')(v'-v) dv' \end{aligned} \quad (21)$$

for the crossing rates,  $P_r$  and  $P_l$ . These crossing rates are identical to what we would expect for a test particle at  $\omega$  having a crossing in a nonuniform bath of  $N$  uncorrelated particles with singlet distribution function  $f(\mu)$ . Because in the real system the total number of particles is fixed, finite size effects will induce correlations, and therefore these forms for the crossing rates will be only approximate.

In order to evaluate  $P_r$  and  $P_l$  for a system with a given stationary Vlasov distribution function we must first find  $\omega$ , the most probable value of  $x$ , by inverting (17). Using (6) in (17) and taking the limit of large  $N$  gives

$$\frac{1}{2}(1-a) = \int_{-\infty}^{\omega} \int_{-\infty}^{\infty} f(x, v) dv dx. \quad (22)$$

This equation directly relates  $\omega$ , the most probable value of  $x$ , to the acceleration. The stationary Vlasov distribution function  $f(\omega, v)$  can then be converted to a function of the acceleration and velocity for use in the general forms for the crossing rates (21).

## B. Derivation of the general Fokker-Planck equations

Since, in the large  $N$  limit, the  $(a, v)$  process for a labeled particle in the OGS is a diffusion, it is governed by a Fokker-Planck equation which determines the evolution of the transition probability and provides a complete statistical model for the system. In the case of the OGS, the transition probability is determined by the probability of one particle crossing another in a small time  $\Delta t$ .

Let  $P(a, v, \tau | a_0, v_0)$  be the transition probability for a labeled particle in the OGS, where we have conditioned on the initial state  $(a_0, v_0)$ . In this system each particle experiences a jump in its acceleration during a crossing while the velocity remains a continuous function of time. As the number of particles in the system goes to infinity and the size of the jumps goes to zero, the acceleration process will move from a jump to a diffusion. Since we wish to examine this diffusive behavior we will take the limit of the increments as  $N \rightarrow \infty$ .

The general form for a two-variable FP equation is

$$\begin{aligned} \frac{\partial P(\vec{z}, \tau | \vec{y}, \tau')}{\partial \tau} &= - \sum_i \frac{\partial}{\partial z_i} [B_i(\vec{z}, \tau) P(\vec{z}, \tau | \vec{y}, \tau')] \\ &+ \sum_{i,j} \frac{1}{2} \frac{\partial^2}{\partial z_i \partial z_j} [C_{i,j}(\vec{z}, \tau) P(\vec{z}, \tau | \vec{y}, \tau')], \end{aligned} \quad (23)$$

where  $P$  is the transition probability for the process. The functions  $B_i$  (the drift vector) and  $C_{ij}$  (the diffusion tensor) are, respectively, the first and second order infinitesimal increments and are the only information required to describe the process. For the  $(a, v)$  process, the infinitesimal increments are defined by

$$K_{\mu, \nu} = \lim_{\Delta \tau \rightarrow 0} \frac{1}{\Delta \tau} \langle (\Delta a)^\mu (\Delta v)^\nu | a, v \rangle. \quad (24)$$

The average in (24) is calculated using the transition probability for the jump process and conditioning on the acceleration and velocity. For a diffusion only the first and second order increments are nonzero. The  $B_i$  and  $C_{ij}$  are then given by

$$B_i = K_{\mu, \nu} \delta_{\mu+v, 1}, \quad C_{i,j} = K_{\mu, \nu} \delta_{\mu+v, 2}. \quad (25)$$

In this section we derive general forms for the infinitesimal increments for an arbitrary stationary Vlasov distribution,  $f(x, v)$ , from which the Fokker-Planck equation governing the  $(a, v)$  process immediately follows. Previously, we derived a general form for the crossing rates of a labeled particle with given initial conditions.

For particle  $j$  in a small time  $\Delta \tau$  there are three possible values for a transition  $\Delta a$ :  $\Delta a = (-2/N, 0, 2/N)$  for a crossing from the right, no crossing, and a crossing from the left, respectively. Equations (21) give the mean rate of crossing from the right and left ( $P_r, P_l$ ). Using (24), the general first order infinitesimal increment of the acceleration is

$$\begin{aligned}
K_{1,0}(a,v) &= \lim_{N \rightarrow \infty} \lim_{\Delta\tau \rightarrow 0} \frac{1}{\Delta\tau} \left[ P_r \Delta\tau \left[ -\frac{2}{N} \right] + P_0 \Delta\tau(0) \right. \\
&\quad \left. + P_l \Delta\tau \left[ \frac{2}{N} \right] \right] \\
&= \lim_{N \rightarrow \infty} \lim_{\Delta\tau \rightarrow 0} \left[ \left[ \frac{2}{N} \right] (P_l - P_r) \right] \\
&\Rightarrow K_{1,0}(a,v) = -2v\rho(\omega), \quad (26)
\end{aligned}$$

where  $P_0 = 1 - (P_r + P_l)$ . The general first order infinitesimal increment of the velocity is

$$K_{0,1}(a,v) = a. \quad (27)$$

All other higher order infinitesimal increments of the  $(a,v)$  process vanish in the Vlasov limit. Therefore the general Fokker-Planck equation governing the evolution of the  $(a,v)$  process is

$$\frac{\partial P(a,v,\tau)}{\partial \tau} = -a \frac{\partial P}{\partial v} - 2v \frac{\partial [\rho(\omega)P]}{\partial a}. \quad (28)$$

This is a Fokker-Planck equation with vanishing diffusion tensor. In the limit that  $N \rightarrow \infty$  we see that there is no diffusion, and the evolution of  $(a,v)$  for a particle in the OGS is deterministic. The solution to (28) is

$$P(a,v,\tau) = \delta(a - a_D) \delta(v - v_D), \quad (29)$$

where  $a_D$  and  $v_D$  represent the deterministic evolution of  $a$  and  $v$ , and  $\omega \rightarrow x_D$  where  $x_D$  is the particle position in the deterministic Vlasov limit. Substitution of (29) into (28) gives a contribution from each  $\delta$  function. For a solution, the coefficients of each must vanish. This gives the following pair of coupled ordinary differential equations for  $a_D$  and  $v_D$  for the stationary system:

$$\frac{da_D}{d\tau} = -2v_D \rho(x_D), \quad \frac{dv_D}{d\tau} = a_D. \quad (30)$$

Thus we have seen that in the Vlasov limit the size of the fluctuations goes to zero as the number of particles approaches infinity. Note, however, that in the discrete system the fluctuations will not vanish for any  $N < \infty$ . In taking the limit of large  $N$  we have washed out the dynamical fluctuations that we wanted to study. In order to see these fluctuations as  $N$  becomes large they must be magnified (scaled). Let  $\xi$  and  $\eta$  represent the scaled fluctuations in the acceleration and velocity about their deterministic limits,

$$\xi = \sqrt{N}(a - a_D), \quad \eta = \sqrt{N}(v - v_D). \quad (31)$$

We now find  $R_{\mu,\nu}$ , the infinitesimal increments of the scaled process  $(\xi,\eta)$ , by again using (24). Since  $a - a_D \cong -2\rho(x_D)(\omega - x_D)$ , the general first order increment of  $\xi$  is

$$\begin{aligned}
R_{1,0}(\xi,\eta) &= \lim_{N \rightarrow \infty} \lim_{\Delta\tau \rightarrow 0} \frac{\sqrt{N}}{\Delta\tau} (\langle \Delta a \rangle - \langle \Delta a_D \rangle) \\
&\Rightarrow R_{1,0}(\xi,\eta) = -2\eta\rho(x_D) + v_D \xi \frac{\partial \ln \rho(x_D)}{\partial x_D}. \quad (32)
\end{aligned}$$

The general first order increment of  $\eta$  is treated similarly and we find

$$\begin{aligned}
R_{0,1}(\xi,\eta) &= \lim_{N \rightarrow \infty} \lim_{\Delta\tau \rightarrow 0} \frac{1}{\Delta\tau} \langle \sqrt{N}(\Delta v - \Delta v_D) \rangle \\
&\Rightarrow R_{0,1}(\xi,\eta) = \xi. \quad (33)
\end{aligned}$$

The general second order increment of  $\xi$  is

$$\begin{aligned}
R_{2,0}(\xi,\eta) &= \lim_{N \rightarrow \infty} \lim_{\Delta\tau \rightarrow 0} \frac{N}{\Delta\tau} [\langle (\Delta a)^2 \rangle + \langle (\Delta a_D)^2 \rangle \\
&\quad - 2\langle \Delta a \rangle \langle \Delta a_D \rangle] \\
&= \lim_{N \rightarrow \infty} \frac{4}{N} (P_r + P_l) \\
&\Rightarrow R_{2,0}(\xi,\eta) = 4 \int_{-\infty}^{\infty} dv' |v_D - v'| f(x_D, v'). \quad (34)
\end{aligned}$$

All other infinitesimal increments of the scaled process are equal to zero. This gives a Fokker-Planck equation with a nonzero diffusion constant for the  $(\xi,\eta)$  process,

$$\begin{aligned}
\frac{\partial P(\xi,\eta,\tau)}{\partial \tau} &= -\frac{\partial}{\partial \xi} [R_{1,0}P] \\
&\quad - \frac{\partial}{\partial \eta} [R_{0,1}P] + \frac{1}{2} \frac{\partial^2}{\partial \xi^2} [R_{2,0}P], \quad (35)
\end{aligned}$$

where  $R_{1,0}$ ,  $R_{0,1}$ , and  $R_{2,0}$  are given by Eqs. (32)–(34). From (35) we see that the  $(\xi,\eta)$  process is a diffusion that characterizes the drift of a labeled particle away from ideal Vlasov behavior. By scaling the fluctuations we have magnified them so that they can be seen and studied. Since  $R_{1,0}$  and  $R_{0,1}$  are functions only of time, and  $R_{2,0}$  does not depend on  $\xi$  or  $\eta$ , (35) belongs to a class of equations known as generalized Ornstein-Uhlenbeck processes whose solutions are known to be bivariate Gaussian [9].

This general form of the Fokker-Planck equation (35) was derived assuming only the statistical independence of the particles. No knowledge of the exact form of the  $N$  body probability distribution function is required to obtain the FP equation governing the diffusion process for a specific initial distribution, only the form of the single-particle distribution function in the Vlasov limit. This approach allows the flexibility needed to study other, perhaps more complicated, stationary nonequilibrium distributions.

#### IV. APPLICATION TO EQUILIBRIUM

To verify our technique and check for consistency, we now apply our general Fokker-Planck equations to the case of the OGS in equilibrium. To do this we need to know the actual form of the Vlasov equilibrium distribution function, which is given above as  $f(x, v) = \theta(v)\rho(x)$ . Substituting  $f(x, v)$  into (22) and inverting gives

$$\omega = -\tanh^{-1}(a). \quad (36)$$

This now gives  $\omega$ , the most probable value of  $x$ , in terms of the acceleration  $a$ . For the discrete system, the actual position  $x$  of a particle will be distributed about  $\omega$ . As the system size  $N$  is increased, the distribution of the position about  $\omega$  will become sharper. Thus

$$\rho(\omega) = \frac{1}{2} \operatorname{sech}^2(\omega) = \frac{1}{2}(1-a^2) \quad (37)$$

and

$$f(\omega, v) = \frac{\pi^{-1/2}(1-a^2) \exp(-v^2)}{2}. \quad (38)$$

After substituting (38) into (21) and integrating, the crossing rate from the right (and similarly the left) becomes

$$P_r = \lambda H(v), \quad P_l = \lambda H(-v), \quad (39)$$

where

$$H(v) = \frac{\pi^{1/2}[v + v \operatorname{erf}(v)] + \exp(-v^2)}{2\pi^{1/2}} \quad (40)$$

and

$$\lambda = \frac{N}{2}(1-a^2). \quad (41)$$

These crossing rates for the OGS in equilibrium agree with those obtained by Miller using the canonical ensemble [8], and again later using the microcanonical ensemble [15], and provide a check on the assumption of statistical independence.

##### A. Fokker-Planck equations for the equilibrium system

We can now use these equilibrium forms for the crossing rates in the general equations governing the  $(a, v)$  and  $(\xi, \eta)$  processes. Using (38) in (28) and (30), the Fokker-Planck equation and the corresponding deterministic equations governing the  $(a, v)$  process are

$$\frac{\partial P(a, v, \tau)}{\partial \tau} = -a \frac{\partial P}{\partial v} - 2avP + v(1-a^2) \frac{\partial P}{\partial a} \quad (42)$$

and

$$\frac{da_D}{d\tau} = -v_D(1-a_D^2), \quad \frac{dv_D}{d\tau} = a_D, \quad (43)$$

where again  $a_D$ ,  $v_D$ , and  $x_D$  represent the deterministic Vlasov evolution of  $a$ ,  $v$ , and  $x$ .

Similarly, we obtain the following Fokker-Planck equation describing the evolution of the scaled  $(\xi, \eta)$  process in equilibrium:

$$\frac{\partial P}{\partial \tau} = -\frac{\partial}{\partial \xi}(GP) - \frac{\partial}{\partial \eta}(\xi P) + \frac{1}{2} \frac{\partial^2}{\partial \xi^2}(DP), \quad (44)$$

where  $D(\tau)$  is the time-dependent diffusion term,

$$D(\tau) = 2(1-a_D^2)[\pi^{-1/2} \exp(-v_D^2) + v_D \operatorname{erf}(v_D)], \quad (45)$$

and  $G(\xi, \eta, \tau)$  is the space- and time-dependent drift,

$$G(\xi, \eta, \tau) = 2a_D v_D \xi - \eta(1-a_D^2). \quad (46)$$

##### B. Moment equations for the equilibrium $(\xi, \eta)$ process

The specific FP equation, (44), governing the  $(\xi, \eta)$  process for the equilibrium ensemble was derived in the preceding section. By conditioning on  $\xi = \eta = 0$  at the initial time  $\tau = 0$ , it provides a tool for investigating the growth of fluctuations in  $(a, v)$  away from idealized Vlasov behavior. To quantify the average deviations from Vlasov behavior at a given time  $\tau$ , it is necessary to derive and solve the ordinary differential equations (ODE's) which govern their behavior. Since the solution of (44) is bivariate Gaussian, all of the information is contained in the first two moments. Define the moments  $L_{\mu, \nu}$  as

$$L_{\mu, \nu} = \langle \xi^\mu \eta^\nu | \tau \rangle, \quad (47)$$

where  $\mu$  and  $\nu$  can take on the values 0, 1, or 2. By multiplying the FP equation by  $\xi^\mu \eta^\nu$  and integrating over  $(\xi, \eta)$ , we obtain the following set of first order coupled ODE's for their evolution:

$$\begin{aligned} \frac{dL_{\mu, \nu}}{dt} &= 2a_D v_D \mu L_{\mu, \nu} - (1-a_D^2) \mu L_{\mu-1, \nu+1} \\ &\quad + \nu L_{\mu+1, \nu-1} + \frac{D}{2} \mu(\mu-1) L_{\mu-2, \nu}, \end{aligned} \quad (48)$$

where  $D$  is given by (45). With the given initial values of  $(0, 0)$ , we see from (48) that the first order moments remain constant at zero.

##### C. Numerical solutions

The general equation (48) provides three coupled equations for the second order moments of the  $(\xi, \eta)$  process. With the addition of Eqs. (43) for the deterministic Vlasov process, they form a set of five coupled ODE's that govern the time evolution of the scaled fluctuations. These equations were integrated numerically. Their solution will be compared in Sec. V to the ensemble average of the fluctuations obtained from the dynamical simulation of an OGS with an initial distribution obtained by sampling the canonical ensemble. Initial conditions that

represent both low and high energy particles were chosen in order to sample very different regions of the  $\mu$  space. The energies are such that the high energy particle does not range too near the ends of the distribution, while the low energy particle does not remain too near the system center for all times. Graphs of the theoretical predictions for the scaled fluctuations are shown in Figs. 1 and 2 for the low energy particle, and Figs. 3 and 4 for the high energy particle. Both long ( $\tau=20$ ) and short ( $\tau=0.5$ ) times are illustrated.

A large amount of structure is seen in the  $\tau=20$  time graphs. In general, as time progresses the fluctuations from Vlasov behavior change periodically while growing larger on the average. The discreteness of the system forces a particle to drift away from its Vlasov image after a short time. It appears that while the test particle is near the center of the distribution its many crossings produce larger deviations in acceleration (smaller in velocity) from Vlasov behavior whereas, away from the center, its fewer crossings result in smaller deviations in acceleration (larger in velocity). This cycle repeats itself as the particle oscillates in the system and produces the “out of phase” appearance of the  $\langle \xi^2 \rangle$  and  $\langle \eta^2 \rangle$  plots. The distinction is magnified for higher energy particles that are able to get far from the center of the distribution where they have fewer crossings than particles of low energy. The fluctuations drop to zero (focus) and then peak again periodically as the particle traverses the system.

## V. NUMERICAL SIMULATIONS

Numerical simulations of the OGS were run on systems of 1000 particles to test the application of the theory to large discrete systems. Simulations were run with initial conditions identical to those used for the theoretical

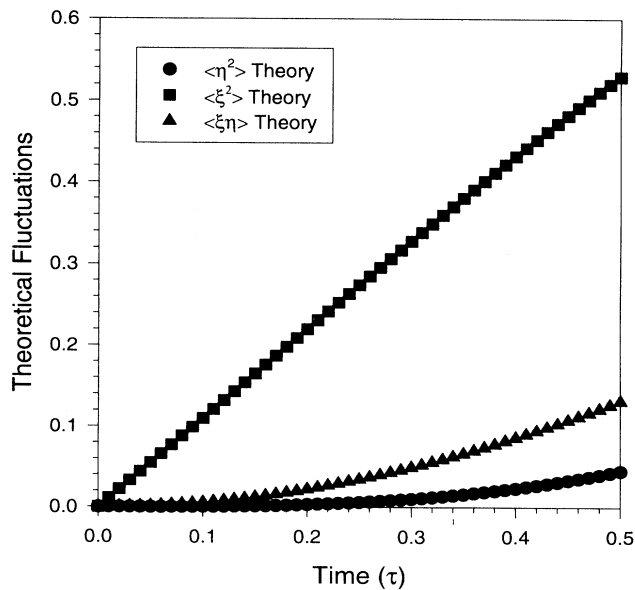


FIG. 1. Growth in time of the scaled theoretical fluctuations away from their Vlasov images during a short time interval ( $\cong 0.1t_c$ ) for a low energy particle.

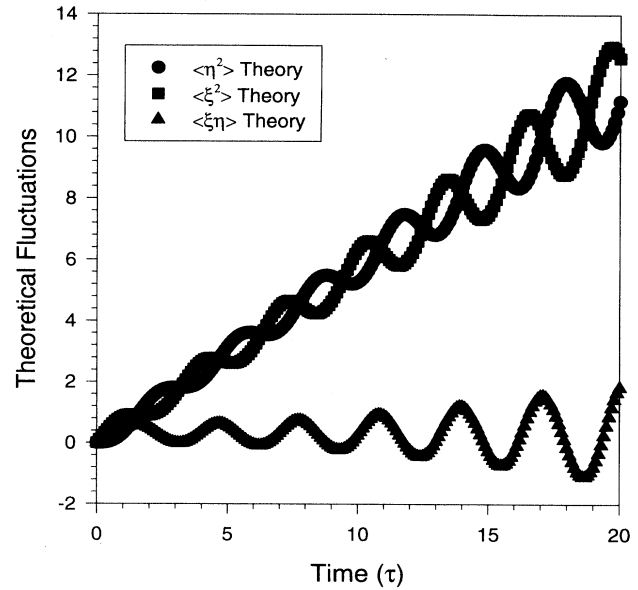


FIG. 2. Growth in time of the scaled theoretical fluctuations away from their Vlasov images during a long time interval ( $\cong 3t_c$ ) for a low energy particle.

predictions, allowing a direct comparison of the simulation results to the theoretical predictions. Statistical data were obtained by conditioning on the acceleration and velocity of a single particle. The acceleration, velocity, and position determine the test particle’s energy. As predicted by the theory, the scaled fluctuations of particles with high and low initial energies show markedly different behavior.

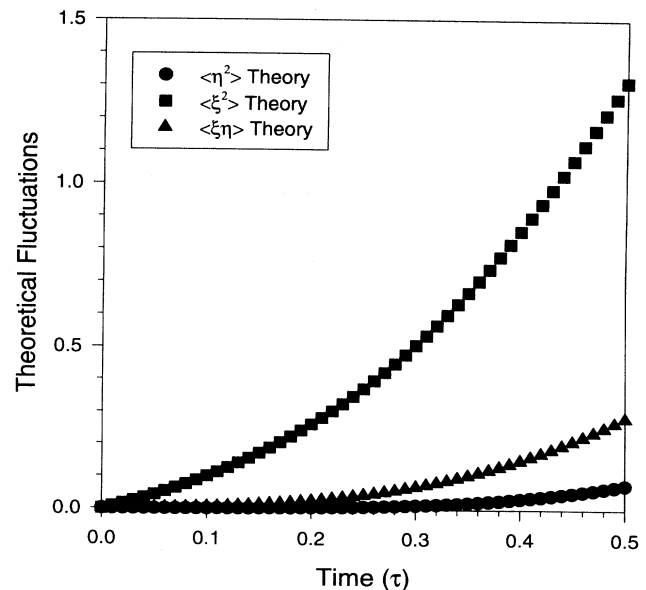


FIG. 3. Growth in time of the scaled theoretical fluctuations away from their Vlasov images during a short time interval ( $\cong 0.1t_c$ ) for a high energy particle.



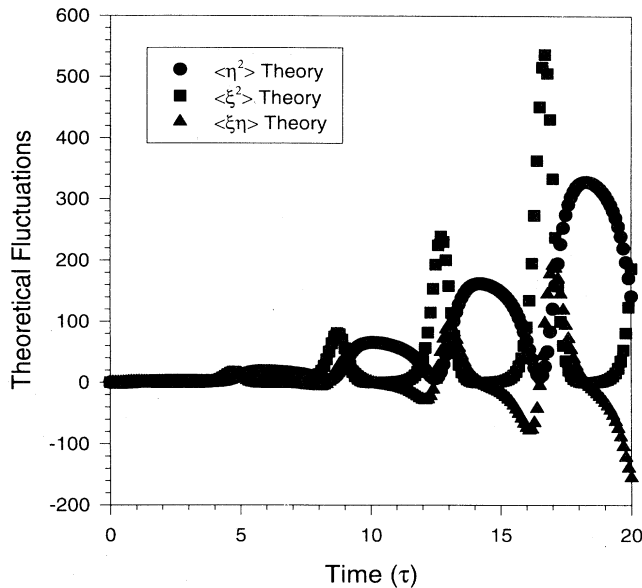


FIG. 4. Growth in time of the scaled theoretical fluctuations away from their Vlasov images during a long time interval ( $\cong 3t_c$ ) for a high energy particle.

To obtain the initial equilibrium state, the test particle's acceleration and velocity are set to the desired initial values. In Eq. (3) we saw that the energy of the system could be written as a sum over nearest neighbor distances. In the canonical ensemble, these nearest neighbor distances are distributed exponentially [12]. With the chosen acceleration and velocity of the test particle, the relative positions of all the particles are found by direct sampling. All positions are then shifted to fix the center of mass at the origin. Levy's method [16] is used to obtain the velocities of the other  $N - 1$  particles of the ordered system from the canonical ensemble under the additional condition that the total momentum be zero.

Numerical simulations of the OGS were run for a total time of  $\tau=20$ . Statistics for the test particle were taken every time it had a crossing with another particle. Position, acceleration, and velocity were recorded as part of the statistical information. In general, a statistical run consisted of an ensemble average of 100 sequential simulations. Each of the simulations began with an initial system in equilibrium obtained independently using the methods described previously. Figure 5 shows a  $\mu$ -space plot of a typical initial system sampled from the equilibrium distribution. The data taken from the test particle during each simulation are stored and the scaled fluctuations from ideal Vlasov behavior are calculated. After the last simulation is complete the fluctuations from ideal Vlasov behavior for each run are averaged. Figure 6 shows a  $\mu$ -space plot of a typical system after a simulation run of  $\tau=20$ . The shapes of the plots before and after the simulation are similar.

Simulation times of  $\tau=20$  should be more than adequate to study the diffusion process. As the system evolves in time, the test particle begins to drift away from

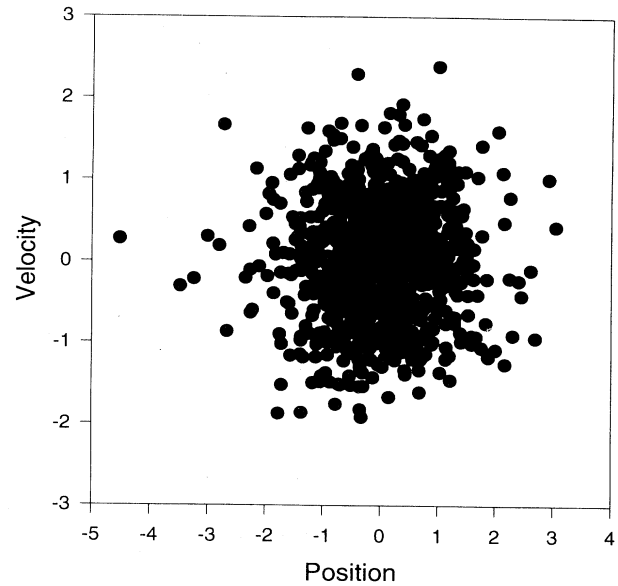


FIG. 5.  $\mu$ -space plot of a typical initial state of the system for a dynamical simulation.

its Vlasov image. For long times the acceleration and velocity of the test particle will be radically different from its Vlasov image. It is not reasonable to expect to identify the test particle with its image after a time sufficient for the fluctuations in a quantity to become comparable to the quantity itself, i.e.,  $\langle \xi^2 \rangle / N \approx \langle a^2 \rangle$  or  $\langle \eta^2 \rangle / N = \langle v^2 \rangle$ . In dimensionless units the variances of acceleration and velocity are of order unity. Therefore an ensemble average of systems sampled from the equilibrium distribution while conditioning on the initial state of

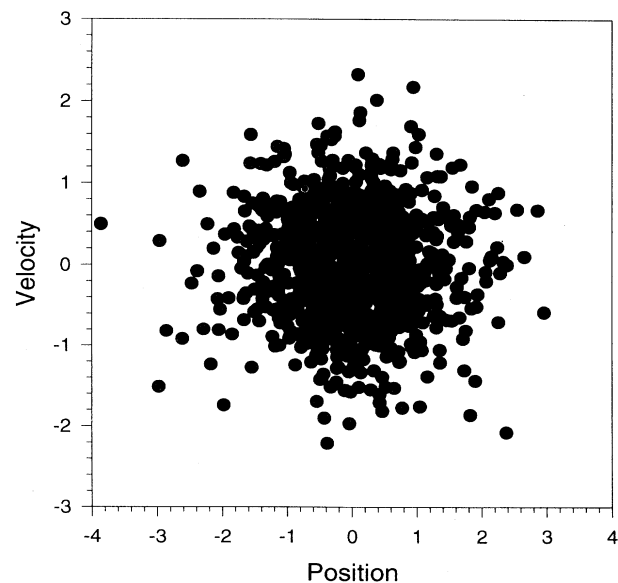


FIG. 6.  $\mu$ -space plot of a typical state of the system at time  $\tau=20$  ( $\cong 3t_c$ ) for a dynamical simulation.

TABLE I. Parameters for conditioned sheets.

Sheet number $j$	Acceleration	Velocity
400	0.201	0.1
100	0.801	0.9

the test particle should at least be modeled successfully by the diffusion process for times such that  $\langle \xi^2 \rangle \ll N, \langle \eta^2 \rangle \ll N$ . Table I lists the initial values of the conditioned particles. All numbers are in scaled (dimensionless) units.

Plots of the average scaled fluctuation in acceleration,  $\langle \xi^2 \rangle$ , of a low energy particle and the theoretical predictions are shown in Figs. 7 ( $\tau=0.5$ ) and 8 ( $\tau=20$ ). Note that the magnitudes compare favorably for very short times as the theory predicts, but tend to start drifting away relatively soon. For  $\tau < 0.25$ , the difference between the simulation and theory is approximately 10% or less. It is surprising that the simulation results and theoretical predictions rejoin, and both the magnitude and phase agree after about  $\tau=17$ . We have not yet determined a satisfactory explanation for this long time effect. The average scaled fluctuation in velocity,  $\langle \eta^2 \rangle$ , and the average scaled fluctuation of the product,  $\langle \xi\eta \rangle$ , exhibit similar behavior and, to conserve space, are not shown.

In Figs. 9 ( $\tau=0.5$ ) and 10 ( $\tau=20$ ) the simulation and theory of the average scaled fluctuation in acceleration,  $\langle \xi^2 \rangle$ , for a high energy sheet are compared. Note the excellent agreement in phase in the long time plots. This appears to be true of the high energy particles in general. However, comparison of the magnitudes reveals a large

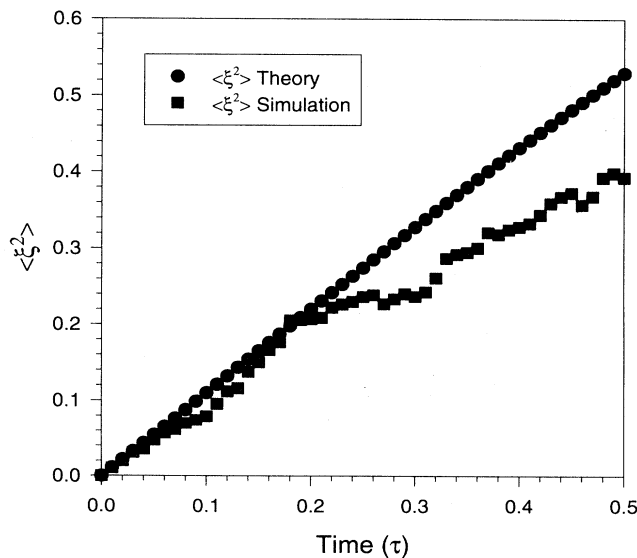


FIG. 7. Comparison of the growth in time of the scaled theoretical variance of the acceleration with the results of the simulation during a short time interval ( $\cong 0.1t_c$ ) for a low energy particle.

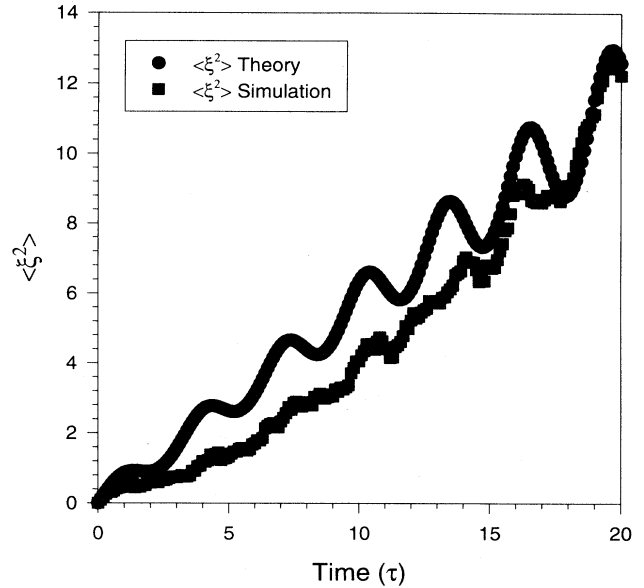


FIG. 8. Comparison of the growth in time of the scaled theoretical variance of the acceleration with the results of the simulation during a long time interval ( $\cong 3t_c$ ) for a low energy particle.

discrepancy: The theoretically predicted average scaled fluctuation is on the order of four times that of the simulation after  $\tau=20$ . For very short times, simulation and theory compare favorably but for longer times they diverge. Again, for  $\tau < 0.25$ , the difference between the simulation and theory is on the order of 10% or less.

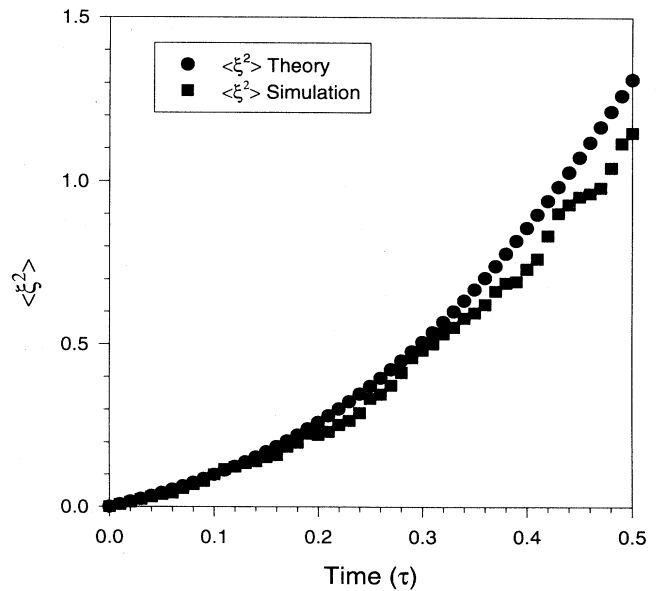


FIG. 9. Comparison of the growth in time of the scaled theoretical variance of the acceleration with the results of the simulation during a short time interval ( $\cong 0.1t_c$ ) for a high energy particle.

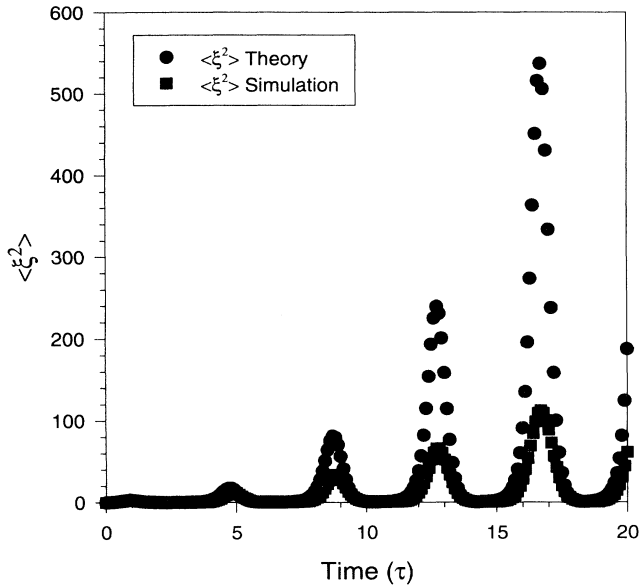


FIG. 10. Comparison of the growth in time of the scaled theoretical variance of the acceleration with the results of the simulation during a long time interval ( $\approx 3t_c$ ) for a high energy particle.

Note also the focusing effect shown by the high energy particle variances as they periodically drop down to zero and then peak to a maximum. As discussed earlier, this effect, predicted by the theory, is confirmed in the simulations. Again, the average scaled fluctuation in velocity,  $\langle \eta^2 \rangle$ , and the average scaled fluctuation of the product,  $\langle \xi \eta \rangle$ , exhibit similar behavior and are not shown.

## VI. CONCLUSIONS

In this paper, dynamical properties of the one-dimensional self-gravitating system were investigated using both analytical methods and computer simulations. Expressions for the crossing rates, infinitesimal increments, and Fokker-Planck equations that govern the  $(a, v)$  and  $(\xi, \eta)$  processes of a labeled particle were derived for an arbitrary initial state corresponding to a stationary solution of the Vlasov equation. These general equations are intended to allow the study of stationary distribution functions other than equilibrium. Simulations of the OGS starting from arbitrary initial conditions show the formation of various quasiequilibrium states,

often long lived, during the evolution of the system. These quasiequilibrium states, for large systems, are believed to be approximate stationary solutions to the Vlasov equation. The diffusion equations derived here for an arbitrary stationary solution may provide a probe to help understand the important dynamical features of these systems as they evolve.

Two main assumptions were used to arrive at the general expressions for the diffusion model. First, a Markov assumption for the jump (acceleration) process that occurs when two particles cross each other was used to introduce stochasticity into the system dynamics. Second, the assumption of statistical independence in the phase space (stosszahlansatz) was used to provide the separability of the phase space distribution function into a product of single-particle functions needed to arrive at simple general forms for the crossing rates. These can be evaluated in turn for any stationary distribution function that satisfies the Vlasov equation. As a check, the general forms for the crossing rates and infinitesimal increments were evaluated for the special case of equilibrium. They were compared with the analytic expressions derived earlier from the more precise equilibrium canonical and microcanonical ensembles, and found to agree exactly.

A thorough test of the diffusion model was undertaken for the special case of equilibrium. Theoretical predictions for the scaled deviations from Vlasov dynamics of the acceleration and velocity ( $\xi$  and  $\eta$ ) were derived and compared to actual dynamical simulations. Results from ensemble averages of 100 dynamical simulations of a finite system of  $N = 1000$  particles agreed with the theory for short times ( $\tau < 0.25$ ) for diffusing particles characterized by both high and low energies. For much longer times, the magnitude of the fluctuations for low energy particles (but not high) generated by the simulations also agreed with the theoretical predictions. In addition, the unusual focusing effect predicted by the theory for higher energy particles was confirmed in the simulations, although the difference in magnitude between theory and simulation at the peaks was quite large. This may indicate the importance of two-particle or higher correlations and collective modes which were neglected by the theoretical assumptions. Further study is required to explain the quantitative differences in the fluctuations between the stochastic theory and simulation. The answer to this question may itself provide insight into the workings of the system dynamics. In future work, the contributions of both two-particle correlations and collective modes to the relaxation process will be investigated.

[1] J. H. Oort, *Bull. Astron. Inst. Neth.* **6**, 289 (1932); G. Camm, *Mon. Not. R. Astron. Soc.* **110**, 305 (1950).  
 [2] L. Cohen and M. Lecar, *Bull. Astron.* **3**, 213 (1968).  
 [3] S. Cuperman, A. Hartman, and M. Lecar, *Astrophys. Space Sci.* **13**, 397 (1971).  
 [4] F. Hohl, Ph.D. thesis, College of William and Mary, 1967; M. Luwel, G. Severne, and J. Rousseeuw, *Astrophys. Space Sci.* **100**, 261 (1984); H. L. Wright, B. N. Miller, and

W. E. Stein, *ibid.* **84**, 421 (1982); C. J. Reidl, Jr. and B. N. Miller, *Astrophys. J.* **318**, 248 (1987); **332**, 616 (1988); **348**, 203 (1990); **371**, 260 (1991); *Phys. Rev. A* **46**, 837 (1988).  
 [5] T. Tsuchiya, T. Konishi, and N. Gouda, *Phys. Rev. E* **50**, 2607 (1994).  
 [6] A. Einstein, *Ann. Phys. (Leipzig)* **17**, 549 (1905).  
 [7] M. v. Smoluchowski, *Ann. Phys. (Leipzig)* **48**, 1103 (1915); A. D. Fokker, *ibid.* **43**, 810 (1914); L. S. Ornstein and G.

- E. Uhlenbeck, *Phys. Rev.* **36**, 823 (1930).
- [8] B. N. Miller, *J. Stat. Phys.* **61**, 291 (1991).
- [9] H. Risken, *The Fokker-Planck Equation*, 2nd ed. (Springer-Verlag, Berlin, 1988).
- [10] N. G. van Kampen, *Stochastic Processes in Physics and Chemistry* (North-Holland, Amsterdam, 1981).
- [11] J. J. Monaghan, *Aust. J. Phys.* **31**, 95 (1978); Y. Fukita and T. Morita, *ibid.* **32**, 289 (1979).
- [12] G. Rybicki, *Astrophys. Space Sci.* **14**, 56 (1971).
- [13] K. H. Prendergast, *Astron. J.* **59**, 260 (1954).
- [14] W. Braun and K. Hepp, *Commun. Math. Phys.* **56**, 101 (1977).
- [15] B. N. Miller (unpublished).
- [16] P. Levy, *Memoir. Sci. Math. Fasc.* (Gauthier-Villas, Paris, 1954), p. 126.